Supplementary Information

Ultrafiltration separation of nanoscale Am(VI)-polyoxometalate clusters from lanthanides

Hailong Zhang[1]†, Ao Li[1]†, Kai Li[1]†, Zhipeng Wang[2], Xiaocheng Xu[3], Yaxing Wang[1]*, Matthew V. Sheridan[1], Han-Shi Hu[3], Chao Xu[2]*, Evgeny V. Alekseev[5], Zhifang Chai[1], Thomas E. Albrecht-Schönzart[4]*, Shuao Wang[1]*

[1]*State Key Laboratory of Radiation Medicine and Protection, School for Radiological and interdisciplinary Sciences (RAD-X) and Collaborative Innovation Center of Radiation Medicine of Jiangsu Higher Education Institutions, Soochow University, Suzhou 215123, China*

[2]*Institute of Nuclear and New Energy Technology, Tsinghua University, Beijing 100084, China*

[3]*Department of Chemistry and Laboratory of Organic Optoelectronics & Molecular Engineering of the Ministry of Education, Tsinghua University, Beijing 100084, China*

[4]*Department of Chemistry and Biochemistry, Florida State University, Tallahassee, Florida 32306, United States*

[5]*Institute of Energy and Climate Research, Forschungszentrum Jülich GmbH, D-52428 Jülich, Germany*

†These authors contributed equally to this work.

Email: yxwang@suda.edu.cn (Y. W.); xuchao@tsinghua.edu.cn (C. X.); tschoenzart@mines.edu (T. E. A.-S.); shuaowang@suda.edu.cn (S. W.).

Preparation of $^{237}Np^{VI}O_2^{2+}$ stock solution. 0.04 M stock solution of $Np^{V}O_2^{+}$ (perchlorate) was obtained first, as shown in Scheme 1. Heating the $Np^{V}O_2^{+}$ solution with the addition of concentrated HNO_3, producing $Np^{VI}O_2^{2+}$ residues. In the heating process, the large excess of NO_2 decomposed from HNO_3 fully oxidizes Np^{V} to Np^{VI}. Then, 0.1 M $Np^{VI}O_2^{2+}$ stock solution was obtained in pink color with the addition of 0.1 M HNO_3, as shown in Scheme 1. The oxidation state of Np was probed by UV-Vis-NIR spectrometry, with the disappearance of the characteristic absorption peak at 980 nm (Np^{V}) and emergence of the characteristic absorption peak of 1200 nm for Np^{VI}.

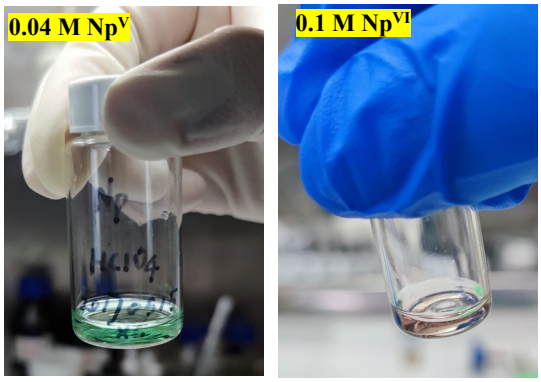

Scheme 1. The stock solution of $^{237}Np^{V}O_2^{+}$ and $^{237}Np^{VI}O_2^{2+}$.

Preparation of $^{242}Pu^{VI}O_2^{2+}$ stock solution. The stock solution of $Pu^{VI}O_2^{2+}$ in nitric acid was prepared by repeatedly dissolving PuO_2 powder in concentrated nitric acid in an autoclave at 200 ^{o}C. Greenish $Pu^{IV}(NO_3)_4$ solutions were obtained followed by distillation in a sand bath at ambient pressure. During this process, HNO_3 decomposes to NO_2, which further oxidizes Pu(IV) to Pu(VI). Then, diluted HNO_3 was added into the residues, obtaining a 0.1 M $^{242}Pu^{VI}O_2^{2+}$ stock solution (Scheme 2).

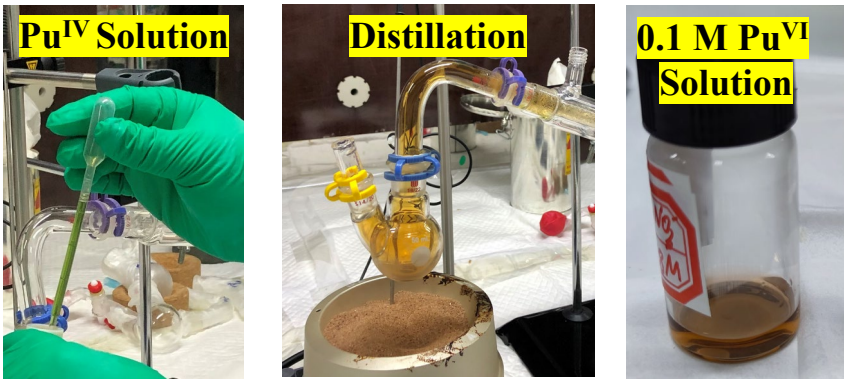

Scheme 2. Preparation of 0.1 M Pu^{VI} solution.

Preparation of $^{243}Am^{VI}O_2^{2+}$ solution. 0.01 M Am(III) solution was obtained by dissolving AmO_2 powder in 0.1 M nitric acid in a vial at room temperature for 3 days. 0.01 M $Am^{VI}O_2^{2+}$ solution was prepared by addition of Cu(III) periodate into the solution of Am(III), in which ~ 99.9 % of the Am(III) was oxidized to Am(VI), monitored by UV-vis-NIR spectroscopy. The solution of $Am^{VI}O_2^{2+}$ was used promptly in the following experiments once in preparation.

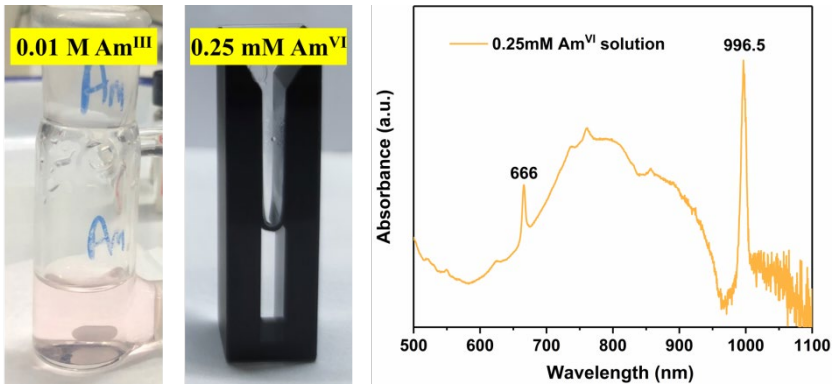

Scheme 3. Preparation of 0.25 mM Am^{VI} solution.

Other characterizations

The Raman spectra of the POM $\{Se_6W_{46}\}$ in the solid-state and in aqueous solutions were recorded using a Confocal LabRAM HR800 spectrometer (Jobin Yvon, France). A laser with an excitation wavelength of 633 nm was used for the measurements in the solid-state. A laser with an excitation wavelength of 514 nm was used for the measurements in aqueous solutions. Elemental analysis (C, H, and N) was performed on a Vario EL CHNOS elemental analyzer. Thermal gravimetric analysis (TGA) was carried out on a NETZSCH STA 449F3 instrument in the range of 30-800 °C under a nitrogen flow at a heating rate of 10 °C min^{-1}. The dynamic light scattering (DLS) was measured with a Zetasizer Nano ZS90 analyzer. The concertation of each element in separation experiments was determined by inductively coupled plasma-mass spectrometry (ICP-MS) for U, inductively coupled plasma optical emission spectrometer (ICP-OES) for Eu, and Quantulus 1220 liquid scintillation counter (Perkin Elmer, USA) for Np, Pu, and Am, respectively.

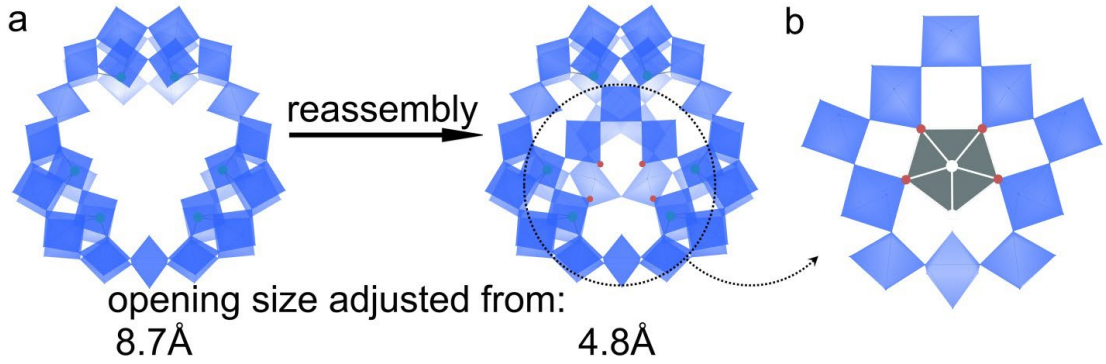

Fig. S1 a, The cluster {Se6W46} was obtained by reassembly of {Se6W39} in acid solution, with the aperture changed from 8.7Å to 4.8Å, forming a new vacancy site. **b**, The vacancy site with four planar oxygen ligands for binding actinyl ions.

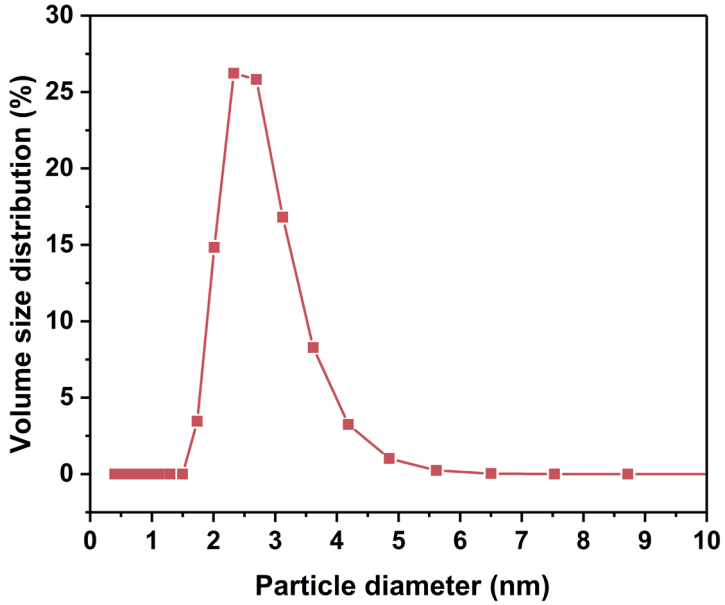

Fig. S2 Volume size distribution on the cluster $\{Se_6W_{46}\}$ (1 mg/mL) in 0.1 M nitric acid solution.

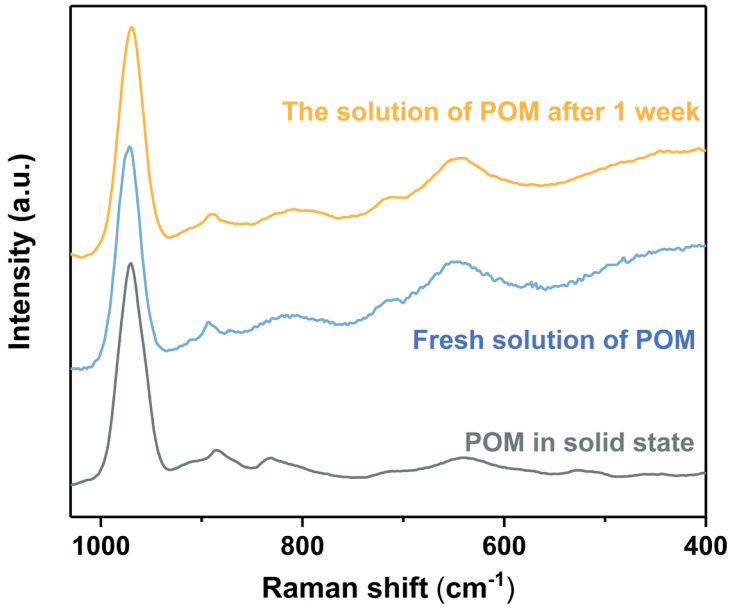

Fig. S3 Raman spectra of $\{Se_6W_{46}\}$ in the solid state and in 0.1 M nitric acid solution (50 mg/mL).

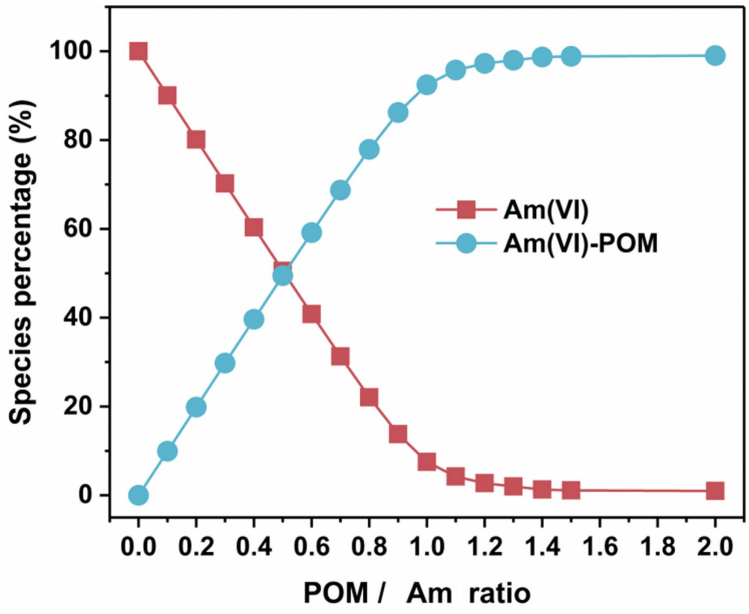

Fig. S4 The species distribution curves as a function of the POM/Am ratio during titration.

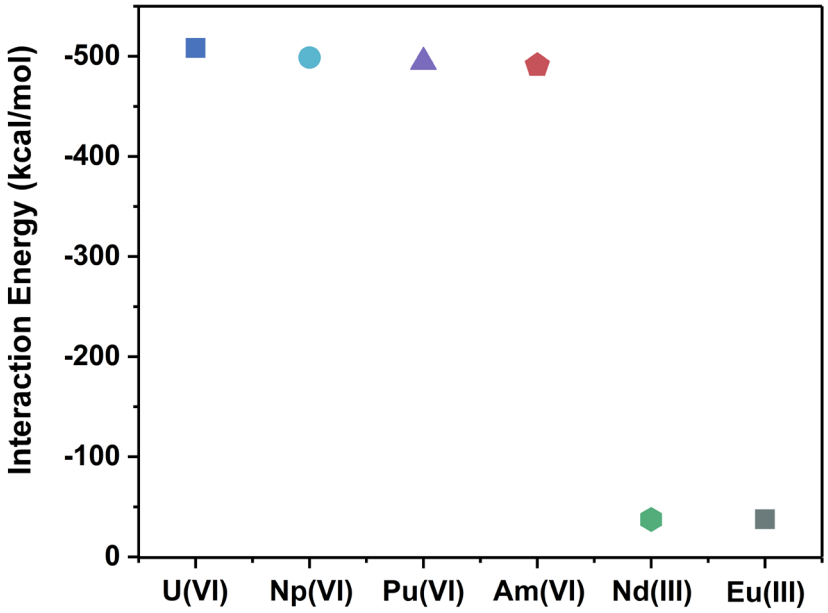

Fig. S5 The calculated total orbital interactions for actinyl-POM and lanthanide ions-POM.

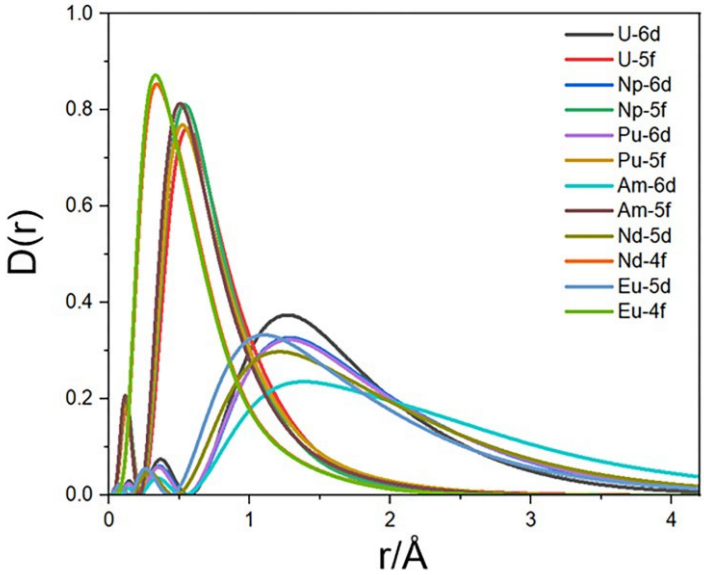

Fig. S6 The radial densities of the 4f atomic orbitals in the lanthanide elements and 5f atomic orbitals of the actinide elements.

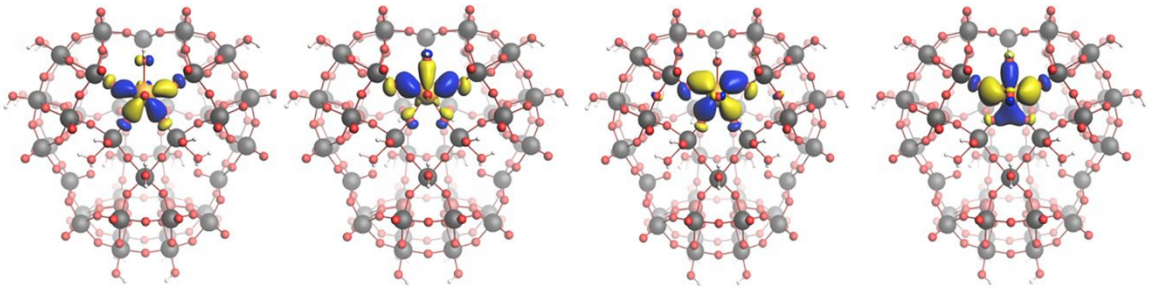

Fig. S7 The energy decomposition analysis of Am(VI)-POM.

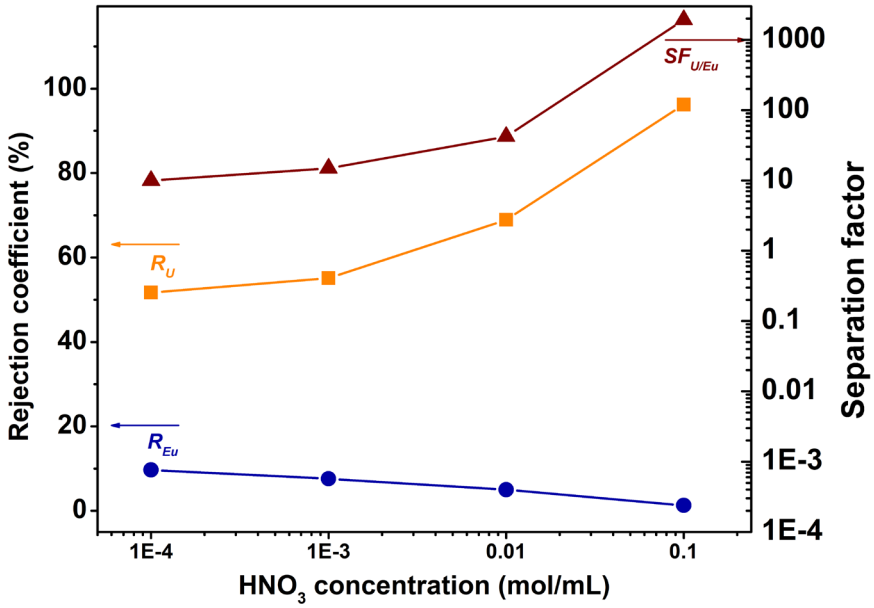

Fig. S8 The influence of acidity on the separation factor (SF) and rejection coefficient (%) for UO_2^{2+}/Eu^{3+} binary separation. The reaction conditions: initial UO_2^{2+} concentration is 2.0 $\times10^{-5}$ mol/L; initial Eu^{3+} concentration is 2.0 $\times10^{-5}$ mol/L; POM concentration is 4.0 $\times10^{-5}$ mol/L; NH_4NO_3 concentration is 0.15 mol/L; reaction time is 5 minutes.

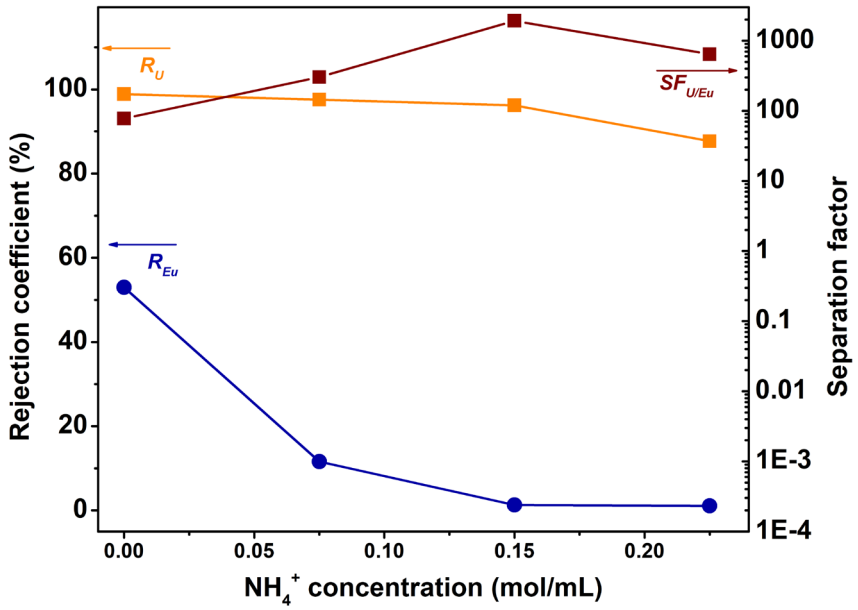

Fig. S9 The influence of NH_4^+ ions on the separation factor (SF) and rejection coefficient (%) for UO_2^{2+}/Eu^{3+} binary separation. The reaction conditions: initial UO_2^{2+} concentration is 2.0 $\times10^{-5}$ mol/L; initial Eu^{3+} concentration is 2.0 $\times10^{-5}$ mol/L; POM concentration is 4.0 $\times10^{-5}$ mol/L; HNO_3 concentration is 0.1 mol/L; reaction time is 5 minutes.

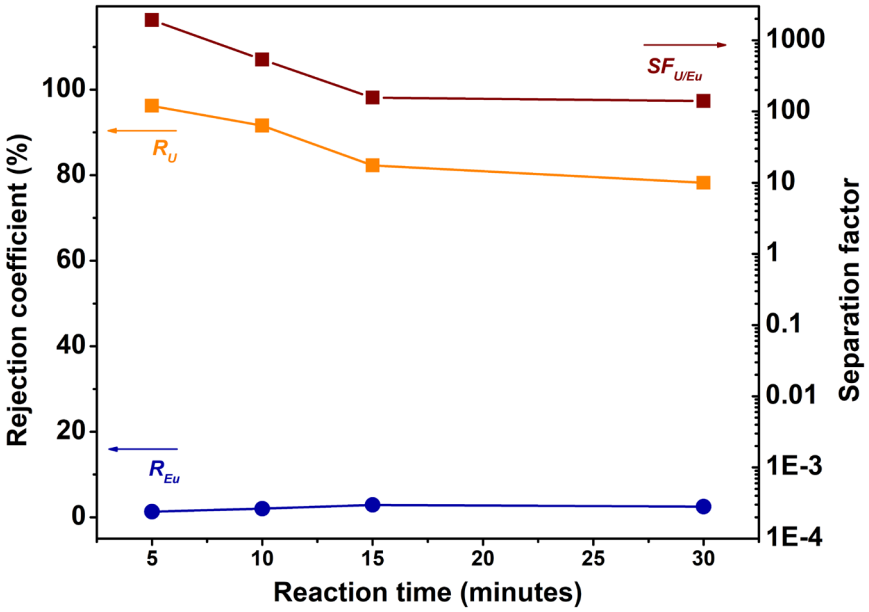

Fig. S10 The influence of reaction time on the separation factor (SF) and rejection coefficient (%) for UO_2^{2+}/Eu^{3+} binary separation. The reaction conditions: initial UO_2^{2+} concentration is 2.0 $\times 10^{-5}$ mol/L; initial Eu^{3+} concentration is 2.0 $\times 10^{-5}$ mol/L; POM concentration is 4.0 $\times 10^{-5}$ mol/L; HNO_3 concentration is 0.1 mol/L; NH_4NO_3 concentration is 0.15 mol/L.

Table S1 Comparisons on the reported values on the binding constant (logβ) between actinyl(VI) ions and inorganic ligands in aqueous solution.

Reaction	logβ	condition	reference
$AmO_2^{2+}+\{Se_6W_{46}\} \rightleftarrows \{AmO_2(Se_6W_{46})\}$	6.00	0.1 M HNO_3	This work
$PuO_2^{2+}+\{Se_6W_{46}\} \rightleftarrows \{PuO_2(Se_6W_{46})\}$	7.26	0.1 M HNO_3	This work
$UO_2^{2+}+F^- \rightleftarrows UO_2F^+$	4.6±0.02	1 mol/L $NaClO_4$	S1
$UO_2^{2+}+SO_4^{2-} \rightleftarrows UO_2SO_4$	2.42	0.2 M $NaClO_4$	S2
	1.88	1 M $NaClO_4$	
$UO_2^{2+}+HSeO_3^- \rightleftarrows UO_2(HSeO_3)^+$	3.35±0.12	0.05 M $NaClO_4$	S3
$UO_2^{2+}+SeO_4^{2-} \rightleftarrows UO_2SeO_4$	1.57±0.01	3 M $NaClO_4$	S4
$UO_2^{2+}+Si(OH)_4 \rightleftarrows UO_2(OSi(OH)_3)^+ + H^+$	-2.92±0.06	0.1 M $NaClO_4$	S5
$UO_2^{2+}+IO_3^- \rightleftarrows UO_2(IO_3)^+$	1.6±0.1	0.05 M $NaClO_4$	S6
$UO_2^{2+}+IO_4^- \rightleftarrows UO_2(IO_4)^+$	1.8±0.2	0.1 M $NaClO_4$	S7
$UO_2^{2+}+PO_4^{3-} \rightleftarrows UO_2PO_4^-$	11.894	0.5 M $NaClO_4$	S8
$UO_2^{2+}+HPO_4^{2-} \rightleftarrows UO_2HPO_4$	6.353	0.5 M $NaClO_4$	
$UO_2^{2+}+H_2PO_4^- \rightleftarrows UO_2H_2PO_4^+$	1.2	3 M HNO_3	S9
$UO_2^{2+}+NO_3^- \rightleftarrows UO_2NO_3^+$	-0.62±0.04	1 M $NaClO_4$	S10
$UO_2^{2+}+HP_2W_{17}^{2-} \rightleftarrows UO_2(HP_2W_{17})$	3.9	0.1 M $HClO_4$	S11
$PuO_2^{2+}+HP_2W_{17}^{2-} \rightleftarrows PuO_2(HP_2W_{17})$	3.3	0.1 M $HClO_4$	
$NpO_2^{2+}+HP_2W_{17}^{2-} \rightleftarrows PuO_2(HP_2W_{17})$	3.4	0.1 M $HClO_4$	

Table S2 Selected bond lengths of An-O in An(VI)-POM.

Bond length summary / Å	U(VI)-POM	Np(VI)-POM	Pu(VI)-POM	Am(VI)-POM
An-O_{yl}1	1.719(2)	1.7196(5)	1.692(2)	1.693(3)
An-O_{yl}2	1.762(3)	1.744(7)	1.713(5)	1.708(2)
An-O_{eq}1	2.322(3)	2.342(7)	2.261(3)	2.379(3)
An-O_{eq}2	2.387(2)	2.420(5)	2.438(4)	2.480(2)
An-O_{eq}3	2.512(3)	2.574(6)	2.438(8)	2.485(3)

Table S3 EDA-NOCV energies of An(VI)-POMs and $Ln(H_2O)_8$ at the PBE/TZ2P/TZP/DZP level.

	U(VI)-POM	Np(VI)-POM	Pu(VI)-POM	Am(VI)-POM	$Nd(H_2O)_8$	$Eu(H_2O)_8$
E_{int}	-508.26	-498.74	-494.46	-491.22	-37.50	-37.74
E_{pauli}	177.25	178.07	165.13	152.97	26.88	25.31
E_{elstat}	-369.67	-369.02	-362.82	-357.48	-13.47	-14.30
E_{orb}	-315.84	-307.79	-296.77	-286.71	-24.03	-23.44

Table S4 Crystal data and structure refinement parameters for An-POM

Compound	Se_6W_{46}	U(VI)-POM	Np(VI)-POM	Pu(VI)-POM	Am(VI)-POM
T(K)	296.15	296.15	120.0	120.0	120.0
Space group	$P2_1/m$	$P2_1/m$	$P2_1/m$	$P2_1/m$	$P2_1/m$
a(Å)	15.6520(10)	14.0224(9)	13.9550(12)	13.6840(11)	13.5104(13)
b(Å)	33.6502(19)	33.595(2)	33.429(3)	33.370(2)	33.262(3)
c(Å)	20.8914(13)	22.9384(15)	22.8155(18)	22.6804(16)	22.8592(19)
α(deg)	90°	90°	90°	90°	90°
β(deg)	98.161(2)	95.202(2)	96.025(4)	96.276(3)	95.555(4)
γ(deg)	90°	90°	90°	90°	90°
V(Å^3)	10891.9(12)	10761.4(12)	10584.6(15)	10294.7(13)	10224.4(16)
Z	2	2	2	2	2
F(000)	9920	9872	10027	9914	10059
Independent reflections	19167	19040	8904	11126	18277
R_{int}	0.0939	0.0882	0.1029	0.1410	0.0715
Completeness	99.4%	98.2%	98.8%	99.0%	99.4%
Goodness-of-fit	1.064	1.030	1.098	1.100	1.048
$R_1[I > 2\sigma(I)]$	0.0974	0.0841	0.1309	0.1279	0.1060
$wR_2[I > 2\sigma(I)]$	0.2470	0.1966	0.2874	0.2765	0.2872
R_1[all data]	0.1727	0.1291	0.1414	0.1624	0.1132
wR_2[all data]	0.3249	0.2268	0.2934	0.2968	0.2942

$R = \Sigma||F_o|-|F_c|| / \Sigma|F_o|$; $wR = \{\Sigma[w(|F_o|^2 - |F_c|^2)^2] / \Sigma[w(|F_o|^4)]\}^{1/2}$

Reference

S1. Tian, G. & Rao, L. Effect of temperature on the complexation of Uranium (VI) with fluoride in aqueous solutions. *Inorg. Chem.* **48**, 6748-6754 (2009).

S2. Geipel, G. *et al.* Uranium (VI) sulfate complexation studied by time-resolved laser-induced fluorescence spectroscopy (TRLFS). *Radiochim. Acta* **75**, 199-204 (1996).

S3. Sladkov, V., Fourest, B. & Mercier, F. Uranyl-Se (IV) interaction in aqueous acid solutions studied by time-resolved laser-induced fluorescence spectroscopy (TRLFS) and UV-Vis spectrophotometry. *Dalton Trans.* **37***,* 7734 (2009).

S4. Lubal, P. & Havel, J. The study of complex equilibria of uranium (VI) with selenate. *Talanta* **44**, 457-466 (1997).

S5. Jensen, M. P. & Choppin, G. R. Complexation of uranyl (VI) by aqueous orthosilicic acid. *Radiochim. Acta* **82**, 83-88 (1998).

S6. Karbowiak, M., Fourest, B., Hubert, S. & Moulin, C. Complexation of U (VI) with iodate ions: determination of stability constants by using spectroscopic methods and capillary zone electrophoresis. *Radiochim. Acta* **91**, 505-512 (2003).

S7. Karbowiak, M., Hubert, S., Fourest, B. & Moulin, C. Complex formation of uranium (VI) in periodate solutions. *Radiochim. Acta* **92**, 489-494 (2004).

S8. Romero-González, M. R., Cheng, T., Barnett, M. O. & Roden, E. E. Surface complexation modeling of the effects of phosphate on uranium (VI) adsorption. *Radiochim. Acta* **95**, 251-259 (2007).

S9. Koma, Y., Aoshima, A., Kamoshida, M. & Sasahira, A. Extraction of Am (VI) from nitric acid solution containing phosphate anion by TBP. *J. Nucl. Sci. Technol.* 39, 317-320 (2002).

S10. Rao, L. & Tian, G. Thermodynamic study of the complexation of uranium (VI) with nitrate at variable temperatures. *J. Chem. Thermodynamics* **40**, 1001-1006 (2008).

S11. Yusov, A. B. & Shilov, V. P. Interaction of U (VI), Np (VI), and Pu (VI) ions with unsaturated heteropolytungstates of the 17th and 11th series in aqueous solutions. *Radiochem.* **49**, 144-151 (2007).